

DUNITE IN LUNAR METEORITE NORTHWEST AFRICA 11421: PETROLOGY AND ORIGIN. A.H. Treiman and J. Semprich, Lunar and Planetary Institute, USRA, Houston TX 77058. <treiman@lpi.usra.edu, jsemprih@lpi.usra.edu>.

Introduction: Dunite is among the rarest lunar lithologies, being represented in the Apollo collection by one macroscopic sample (72415 [1-3]) and a few clasts in polymict breccias [4,5]. Known lunar dunites are related to the Mg-suite plutonic rocks [5], but the uppermost lunar mantle is also inferred to be magnesian dunite [6,7]. Thus, any new lunar dunite sample, mantle or not, would be an important find. Here, we report an olivine rich lithic clast in the lunar meteorite NWA 11421, and infer it to be from the lunar mantle.

Sample & Methods: A fragment of Northwest Africa (NWA) 11421, 11.67 gram, was purchased from M. Cimala (Polandmet.com). Its properties are consistent with the official meteorite description. NWA 11421 is inferred to be part of a large pairing group with NWA 8046 and many others [8]. The meteorite is an impact melt breccia, with mineral and lithic fragments (most from anorthosite and troctolite) in dense black glass [9]. The olivine-rich clast studied here (Fig. 1) was noted on a weathered surface, and its extent determined with X-ray computed tomography [9].

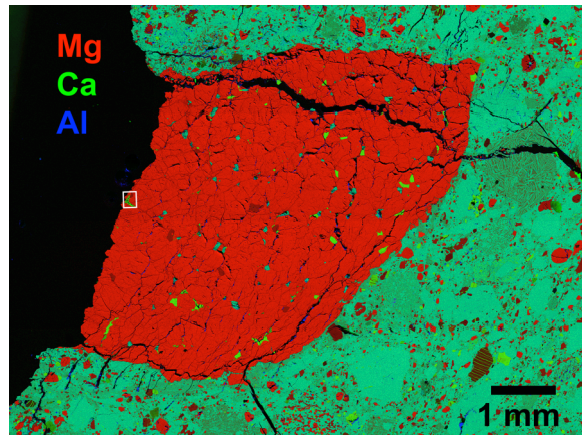


Figure 1. SEM-EDX false color element map of the dunite clast. Olivine is bright red; low-Ca pyroxene is dull red; augite is bright green; plagioclase is bluish green, chromite is black. Epoxy to left (black); impact melt breccia (light green with multicolored spots) surrounds the dunite.

Modal Mineralogy. Mineral abundances in the olivine-rich clast were determined from EDS X-ray maps, taken with the JEOL 7600 SEM at ARES division, Johnson Space Center. Using the Multispec[®] program, training areas for minerals were established on maps of MgK α , CaK α , FeK α , CrK α , and SiK α ; mineral abundances were then retrieved using a maximum likelihood classifier [10].

Mineral Analyses. Chemical analyses were obtained with the JEOL 8530 FEG microprobe at ARES: accelerating potential 15 kV, with the beam at 30 nA and 1 μ m diameter. Count times were 60 sec on peak for Ti, Al, Cr, and Na; others were 30 or 40 sec. Standards were well-characterized oxides and minerals. Data reduction was via the JEOL PRZ routine.

Thermobarometry. Temperatures were calculated with a two-pyroxene thermometer [11] from adjacent augite-orthopyroxene pairs assuming uncertainties of ± 20 $^{\circ}$ C (1 σ). Pressures were obtained with the average P method [12] for assemblages clinopyroxene (augite) + olivine + plagioclase \pm chromite using improved thermodynamic models [13]. Uncertainties in pressure are propagated through from analytical uncertainties in the compositional variables and uncertainties in end-member activities.

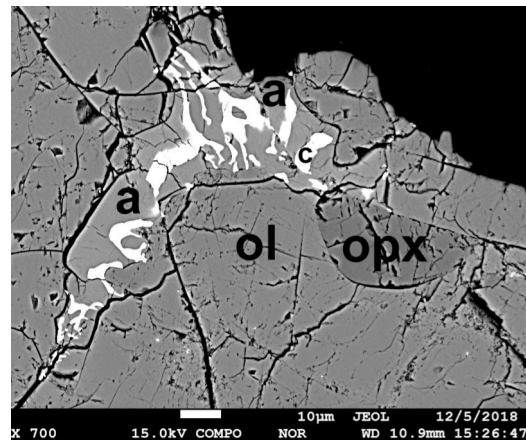


Figure 2. BSE image of symplectite of augite (a) and chromite (c) in olivine (ol) with low-Ca pyroxene (opx). Epoxy to top right; this area is in box on Fig. 1.

Petrography: The olivine-rich clast, Fig. 1, is dunite, and contains (by volume) 95.3% olivine, 1.6% low-Ca pyroxene; 1.1% augite; 1.3% plagioclase, and 0.7% chromite; a single 5 μ m grain of Fe sulfide is present. The pyroxenes show no exsolution lamellae. No ilmenite, armalcolite, or metal is present. Mineral grains are typically 100 to 200 μ m across. The texture is granular, with many 120 $^{\circ}$ grain junctions and no obvious preferred orientation. Some augite grains are elongated; they lie among and partially enclose olivine grains, and many are in symplectic intergrowths with chromite (Fig. 2). In the symplectites, grains range from 5 to <1 μ m (Fig. 2). Terrestrial alteration is limited to rare calcite and clay (identified by presence of K, Al, Mg, & Fe) along cracks.

Table 1. EMP Mineral Compositions

oxide	Pl	Oliv	Aug isol	Opx isol	Aug OCP3	Opx OCP3
SiO ₂	44.02	39.81	52.03	55.57	52.59	55.20
TiO ₂	0.01	0.02	1.33	0.53	1.06	0.69
Al ₂ O ₃	35.90	0.02	2.41	1.39	1.91	1.53
Cr ₂ O ₃	0.00	0.04	0.89	0.58	0.75	0.64
FeO	0.69	16.01	4.52	10.06	4.27	9.93
MnO	0.01	0.20	0.13	0.20	0.12	0.20
MgO	0.11	44.56	17.16	30.80	17.18	30.52
CaO	19.20	0.04	21.33	1.35	22.18	1.57
Na ₂ O	0.38	0.01	0.07	0.01	0.04	0.00
Sum	100.33	100.71	99.86	100.48	100.09	100.29

Plagioclase (Pl) and olivine (Ol) compositions are essentially identical across the whole dunite clast. The OCP3 analyses are grains of augite (Aug) and low-Ca pyroxene (Opx) in contact. 'isol' grains are not in contact with other pyroxenes.

Mineral Compositions: Mineral compositions are given in Table 1. Plagioclase is An_{96.5} and olivine has Mg#~83.5 and FeO/MnO~80; both are consistent with those of lunar Mg-suite dunites [5]. Pyroxene compositions vary, depending on whether they are isolated grains or adjacent to other pyroxenes, plagioclase, and chromite (Table 1).

Equilibration Conditions: Pressures and temperatures of equilibration (Fig. 3) were calculated for several opx and aug grains in contact, with the common pl, oliv, and chromite. Temperatures come mostly from Ca distribution between pyroxenes; pressures derive from a set of independent reactions, mostly involving the Al contents of pyroxenes, among end-members of pyroxenes, olivine, plagioclase, and spinel [13].

The uncertainties shown on Fig. 3 are 1 σ of the calibrations [11-13]; considering all the aug-opx pairs, we adopt an average pressure of 3.75 kbar \pm 2.25 kbar 2 σ . This range corresponds to depths in the Moon of ~67.5 \pm 40 km 2 σ .

Interpretation: The NWA 11421 dunite is distinct from other lunar dunites. **I.** 72415, the only large lunar dunite, is a cataclastic breccia [1-3] with olivine grains to ~2 mm. It does contain chromite-augite symplectites, but also apatite-rich veins (which NWA 11421 does not). **II.** A14 regolith contains dunite fragments, 2-4 mm across [14-16], but most are likely cataclased and recrystallized fragments from troctolites. **III.** Dunite xenoliths in High-Ti basalt 74275 are interpreted as olivine cumulates from High-Ti basalt magmas [5], and are texturally and chemically distinct from the NWA11421 dunite.

From the formation depth inferred from mineral equilibria, the source of the NWA 11421 dunite could have been in either the lunar mantle or crust, which ranges from zero to ~65 km thick [17]. From depth alone, a mantle origin seems likely. The dunite's

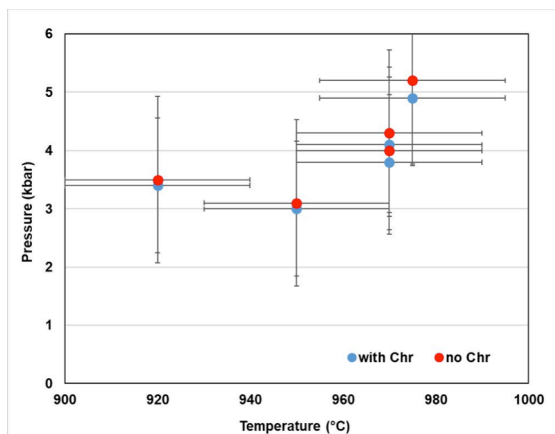


Figure 3. Calculated equilibration conditions for the observed mineral assemblage. Temperatures from a two-pyroxene thermometer, pressures from average P calculations for assemblage with and without chromite (blue/red).

chemical composition is consistent with either upper mantle peridotite [6,7] or cumulates from crustal intrusions [1,5]. For either source, the dunite's equilibration T is far above that of the present-day lunar geotherm, suggesting either a very ancient equilibration or formation in a thermal anomaly (i.e., from an igneous intrusion or a major impact event). The dunite's texture (Fig. 1), fine grained granular, is unlike that of a typical igneous cumulate (not granular) or of a terrestrial mantle peridotite (coarser-grained). The texture resembles that of a recrystallized mylonite or pseudotachylite (e.g. [18,19]), such as might form as a mantle or cumulate dunite was deformed and recrystallized by the shear and heat of an asteroidal impact. Thus, we provisionally interpret the dunite in NWA 11421 as a highly tectonized and recrystallized fragment of the Moon's upper mantle.

Acknowledgments: K. Ross and C. Goodrich assisted with EMP analyses. D. Coleff and R. Ziegler assisted with the CT scan. Supported in part by the CLSE node of SSERVI (D. Kring, PI).

References: [1] Ryder G. (1992) *Proc. LPSC* 22, 373-380. [2] Meyer C. (2011) 72415, in *Lunar Sample Compendium*. [Web link](#). [3] Dymek R.F. et al. (1975) *Proc. LSC* 6th, 301-341. [4] Warren P.H. (1993) *Am. Min.* 78, 360-376. [5] Shearer C.K. et al. (2015) *Am. Min.* 100, 294-325. [6] Shearer C.K. & Papike J.J. (1999) *Am. Min.* 84, 1469-1494. [7] Elkins-Tanton L. et al. (2002) *EPSL* 196, 239-249. [8] Korotev R. (2019) [web link](#). [9] Treiman A.H. et al. (2018) *MaPS* 53, A314. [10] Maloy A.K. & Treiman A.H. (2007) *Am. Min.* 92, 1781-1788. [11] Brey G.P. & Köhler T. (1990) *J. Petrol.* 31, 1353-1378. [12] Powell R. & Holland T.J.B. (2004) *Am. Min.* 79, 120-133. [13] Ziberna L. et al. (2017) *Am. Min.* 102, 2349-2366. [14] Morris R.V. et al. (1990) *Proc. LPSC* 20th, 61-75. [15] Goodrich C.A. (1986) [16] Lindstrom M.M. et al. (1984) *Proc. LPSC* 15th, C41-C49. [17] Wiczorek M.A. et al. (2013) *Science* 339, 671-675. [18] Matysiak A.K. & Trepman C.A. (2015) *Tectonics* 34, 2514-2533. [19] Treiman A.H. (1998) *MaPS* 33, 753-746.